Supporting Information

Optical source apportionment and radiative forcing of light-absorbing carbonaceous aerosol at a tropical marine monsoon climate zone: the importance of ship emissions

Qiyuan Wang[1,2], Huikun Liu[1], Ping Wang[3], Wenting Dai[1], Ting Zhang[1], Youzhi Zhao[3], Jie Tian[1], Wenyan Zhang[1], Yongming Han[1,2], Junji Cao[1,2]

[1]Key Laboratory of Aerosol Chemistry and Physics, State Key Laboratory of Loess and Quaternary Geology, Institute of Earth Environment, Chinese Academy of Sciences, Xi'an 710061, China

[2]CAS Center for Excellence in Quaternary Science and Global Change, Xi'an 710061, China

[3]Hainan Tropical Ocean University, Sanya 572022, China

■ **Contents of this file**

Table S1. The average mass concentrations of carbonaceous matter, water-soluble ions, inorganic elements, and organics during the campaign.

Types	Species	Average	Standard deviation
Carbonaceous matter ($\mu g\ m^{-3}$)	organic carbon	2.71	1.05
	elemental carbon	0.78	0.27
Water-soluble ions ($\mu g\ m^{-3}$)	Na^+	0.49	0.19
	NH_4^+	0.61	0.37
	K^+	0.17	0.09
	Mg^{2+}	0.05	0.02
	Ca^{2+}	0.22	0.17
	Cl^-	0.25	0.18
	NO_3^-	0.62	0.28
	SO_4^{2-}	3.45	1.15
Inorganic elements ($ng\ m^{-3}$)	Ti	13.08	9.65
	V	2.36	1.39
	Mn	5.13	2.65
	Fe	127.36	78.99
	Ni	1.07	0.65
	Cu	28.00	14.40
	Zn	16.58	11.10
	Br	2.62	2.02
Organics ($ng\ m^{-3}$)	hopanes	0.17	0.05

Table S2. The average aerosol light absorption contributed by primary emissions ($Abs_{pri}(\lambda)$) and secondary formation (($Abs_{sec}(\lambda)$)) during the campaign. λ represents the wavelength of 370, 470, 520, 590, 660, or 880 nm.

Light absorption	Average (Mm^{-1})	Standard deviation (Mm^{-1})
$Abs_{pri}(370)$	14.9	8.6
$Abs_{pri}(470)$	10.8	5.7
$Abs_{pri}(520)$	9.1	4.7
$Abs_{pri}(590)$	7.8	4.0
$Abs_{pri}(660)$	6.6	3.3
$Abs_{pri}(880)$	4.7	2.3
$Abs_{sec}(370)$	0.8	1.8
$Abs_{sec}(470)$	0.5	0.9
$Abs_{sec}(520)$	0.4	0.7
$Abs_{sec}(590)$	0.3	0.6
$Abs_{sec}(660)$	0.2	0.4

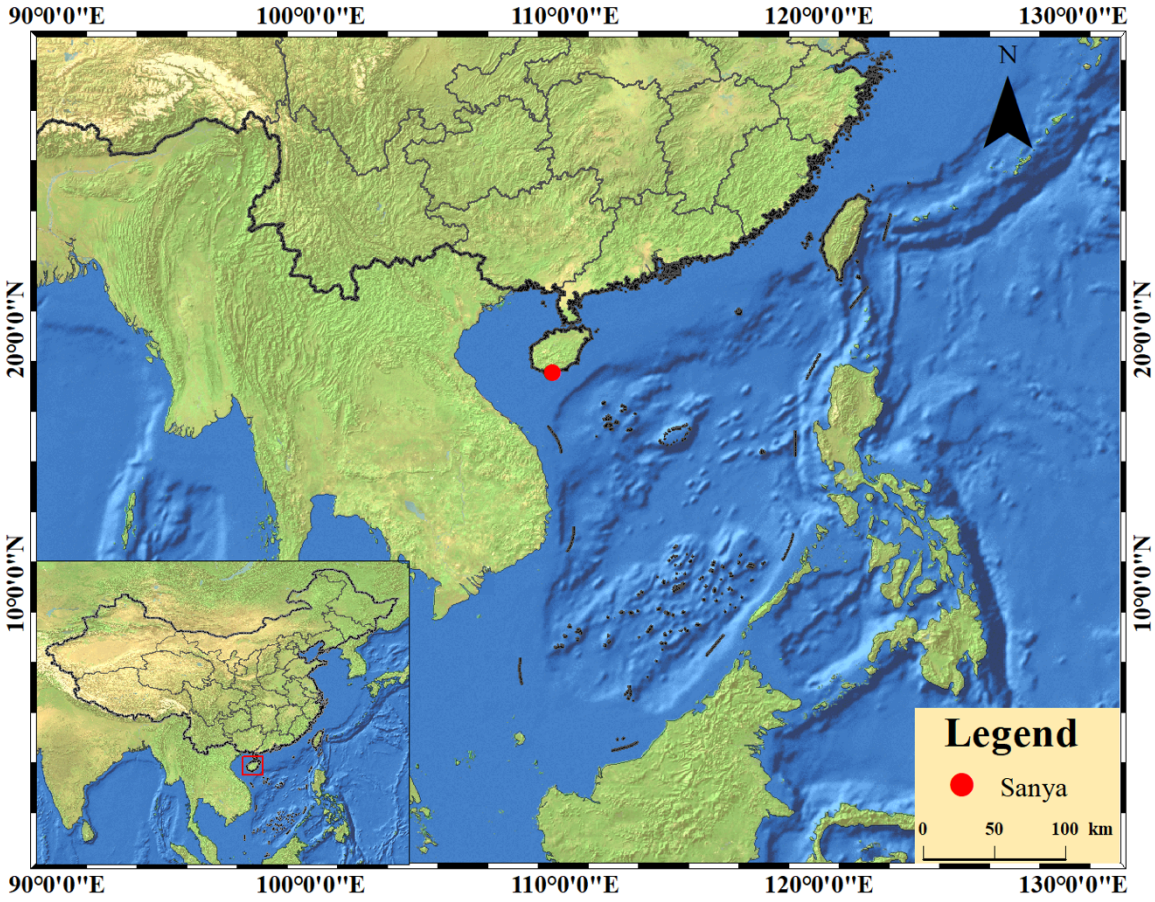

Figure S1. Map showing the Sanya sampling site and surrounding areas. The map was drawn using ArcGIS software. The base map is the World Topographic Map from © ESRI (Environmental Systems Research Institute, Inc.) (www.arcgis.com/home/item.html?id=30e5fe3149c34df1ba922e6f5bbf808f).

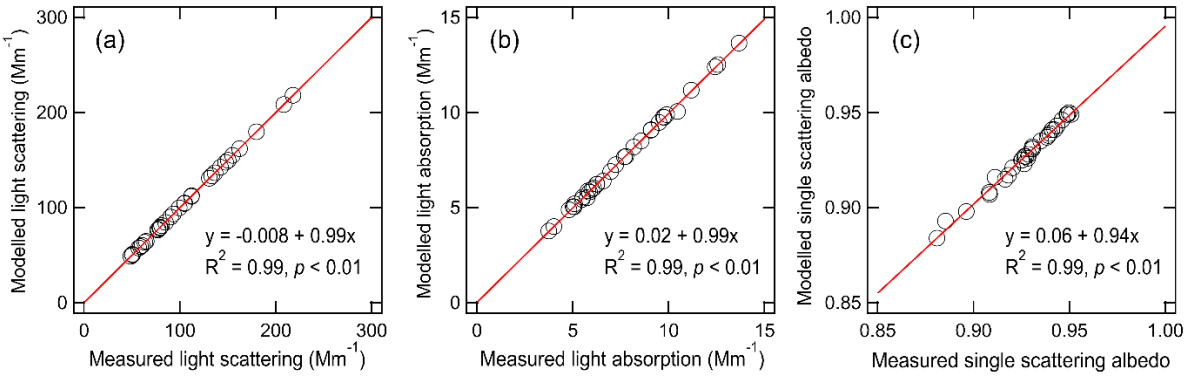

Figure S2. Scatter plots of optical parameters modelled with Optical Properties of Aerosol and Cloud model versus values measured with a photoacoustic extinctiometer.

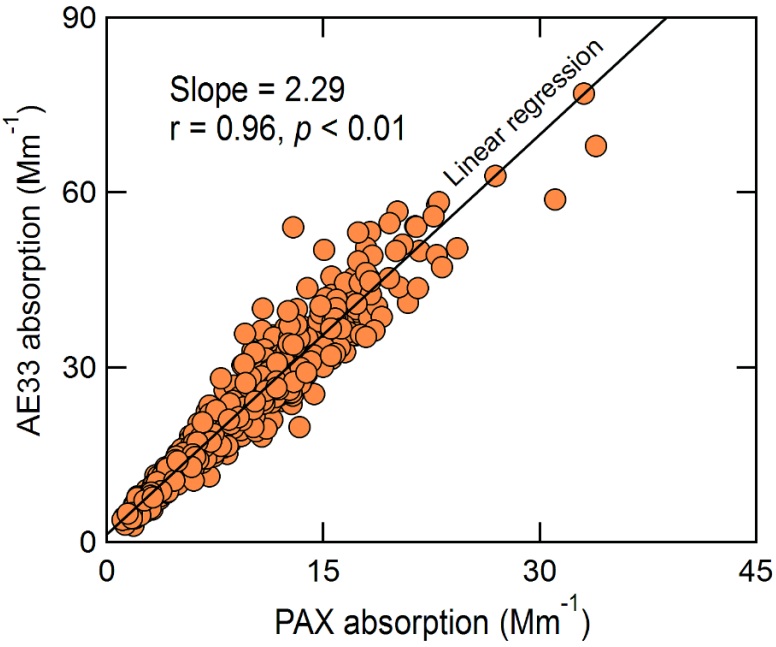

Figure S3. Relationship between the light absorption coefficient measured by model AE33 aethalometer at wavelength of 520 nm and photoacoustic extinctiometer (PAX) at wavelength of 532 nm.

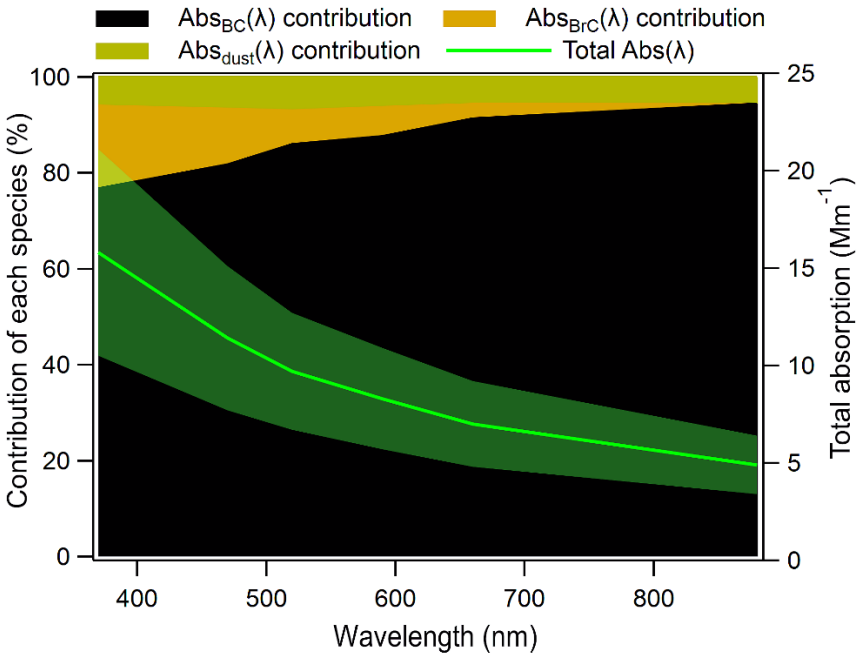

Figure S4. The distributions of total aerosol light absorption coefficients at different wavelengths of 370, 470, 520, 590, 660, and 880 nm and its contributions from black carbon (BC), brown carbon (BrC), and mineral dust. The $Abs_{BC}(\lambda)$, $Abs_{BrC}(\lambda)$, and $Abs_{dust}(\lambda)$ are the light absorption contributed by BC, BrC, and mineral dust, respectively. The green shadow represents one standard deviation of total aerosol light absorption coefficients.

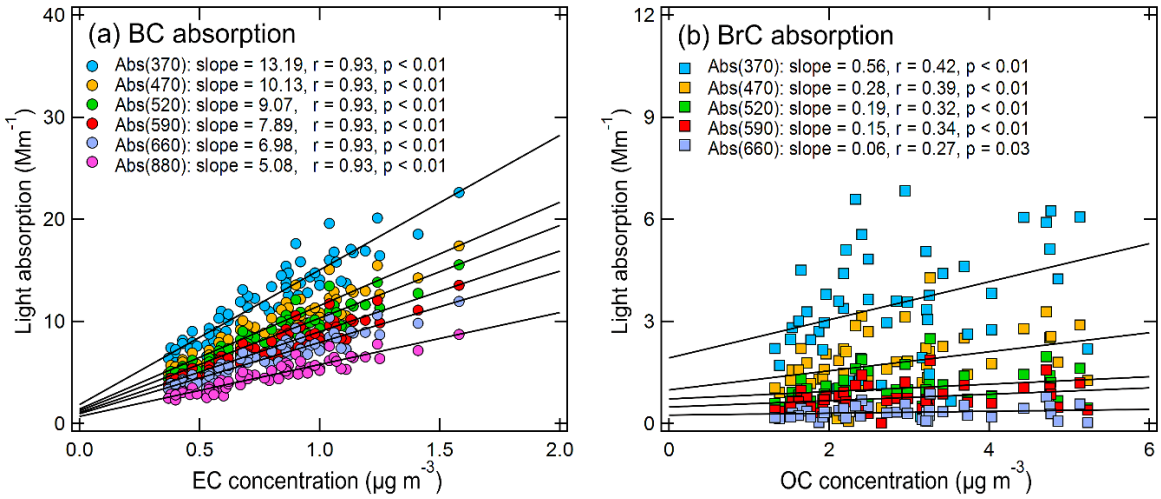

Figure S5. Scatter plots of (a) light absorption of black carbon (BC) versus mass concentration of elemental carbon (EC) and (b) light absorption of brown carbon (BrC) versus mass concentration of organic carbon (OC). The black lines are the linear regression.

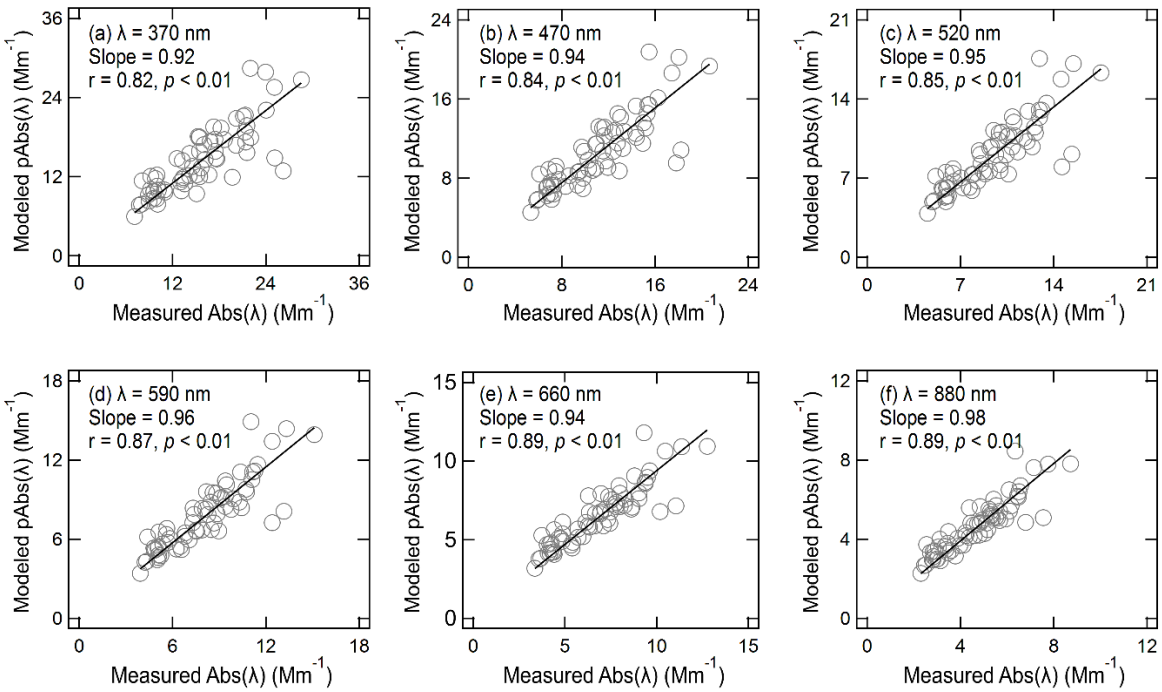

Figure S6. Scatter plots of primary light absorption (pAbs(λ)) simulated with a positive matrix factorization model versus light absorption (Abs(λ)) measured with a multi-wavelength aethalometer. λ represents wavelength of 370, 470, 520, 590, 660, or 880 nm.